

Modeling and Simulation of Wake Encounter for a Fighter Aircraft

**C Kamali¹, Abhay Pashilkar¹, N Indira², Anup Goyal², Premalatha³
and Vidyadhar Mudkavi[#]**

¹Scientist, Flight Mechanics & Control Division, CSIR-NAL, Bangalore 560017,
{ckamali@nal.res.in, apash@nal.res.in}

²Scientist, Aerodynamics and Performance Directorate, ADA, Bangalore 560017,
{indira@jetmail.ada.gov.in, anup.goyal0@gmail.com }

³Scientist, Computational & Theoretical Fluid Dynamics Division, CSIR-NAL,
Bangalore 560017, {vm@ctfd.cmmacs.ernet.in,
mailto:prema@ctfd.cmmacs.ernet.in}

Abstract

This paper addresses the development of six degrees of freedom model for simulation of flight in the wake of a similar class aircraft. The aircraft considered in this study is a high performance fighter with full authority flight control laws. Apart from the aerodynamic effects, the flight dynamic model also includes a model of the air data system and the feedback control laws. The model is used to study the effect of wake on the flight dynamic response of the aircraft with and without effect of wake on the air data system feedback variables like angle of attack, angle of sideslip and static pressure.

Nomenclature

B_L	Distance between the vortices
C_X	Axile force coefficient
C_Y	Side force coefficient
C_Z	Vertical force coefficient
C_l	Rolling moment coefficient
C_m	Pitching moment coefficient
C_n	Yawing moment coefficient
CG	Follower Aircraft Center of gravity
DCM	Direction Cosine Matrix
r_c	Core diameter
\vec{r}	Position vector
u, v, w	Aircraft inertial velocities in body frame
α	Angle of attack
β	Angle of side slip
δC_{wake}	Incremental aerodynamic coefficient due to wake
Γ	Vortex strength

1. INTRODUCTION

Modern fighters are designed to be unstable to attain high maneuverability and are augmented with full authority control laws. As a consequence of lift, every aircraft sheds wake in the form of vortex sheet which eventually rolls up into one or more pairs of filament-like structures known as the trailing vortices [1-3]. Although wake poses significant hazard and is well studied area, a complete understanding of this phenomena still eludes us. During training and air combat scenarios, there is a high probability of encountering wake of other aircraft flying ahead. Recent experiences of modern fighters have shown that wake encounters result in critical problems such as [4]:

- Airframe vibration followed by structural failure due to eigen-mode excitation.
- Serious departure tendencies.
- Exceedence of g limits.
- Violent disturbances in roll.
- Engine flameouts for short duration.

- Loss of control caused by adverse aerodynamics and sensor behavior due to wake encounters.

When Boeing 747 was inducted into service in 1970, the wake problem became significant in terminal operations. In 1970, SAAB 37 Viggen's upper part of the vertical fin was lost because of a likely wake encounter. Subsequent aero elastic analysis verified this incident [4]. In 1999, SAAB 39 Gripen was lost in connection with wake vortex encounter while practicing air combat [4]. In 2001, an Airbus A300's fin was ripped off in a likely wake encounter [4]. After a number of Wake Vortex related incidents in Swedish Air Force service, it was decided to conduct modeling and simulation studies of a wake vortex encounter. This capability was used to design better control characteristics through more than 12000 wake vortex passage simulations [5]. In this paper, six degrees of freedom simulation model is developed and discussed to study the effects of wake of one fighter aircraft on another aircraft of the same type.

2. MODEL REQUIREMENTS

The generic wake encounter concept is shown in figure 1. The simulation model developed for the wake encounter concept meets the following requirements:

- Leader aircraft-A for wake vortex generation.
- Follower aircraft-B for experiencing the wake.
- Wake vortex model for the induced velocity profile experienced by aircraft-B.
- Incremental aerodynamic interactive model due to wake for aircraft-B.
- Air data system model for aircraft-B.
- Nominal six DOF model for the aircraft-B.
- Control laws for aircraft-B.

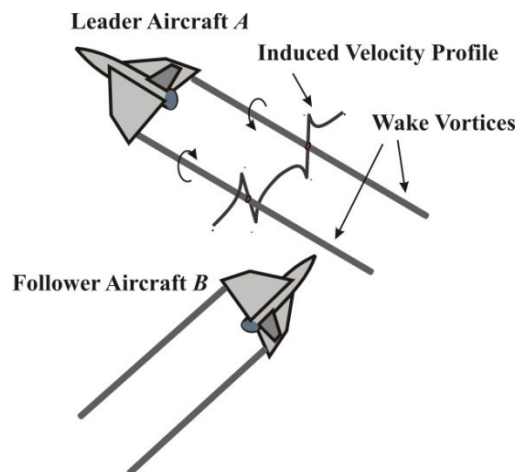


Figure 1. Generic wake encounter concept.

3. WAKE VORTEX MODEL

A finite lifting surface, such as a wing, sheds vorticity in its wake in the form of a thin vortex sheet which is highly unstable. The vortex sheet rolls up into one or more pairs of tube-like counter rotating structures known as the trailing vortices. The roll up process happens quickly in a few span lengths. The roll up process together with viscous effects results in a well defined core that rotates like a solid body. The trailing vortex induces a velocity field around it which can be calculated using the Biot-Savart law. The trailing vortices themselves distort owing to disturbances which persist in the atmosphere. In general, one can neglect the longitudinal distortions and make a reasonable assumption that the vortices behave like two-dimensional structures, i.e., the axis of the vortices is nearly straight. If we fix the origin of axes at the center of one of the trailing vortex, then the induced velocity $v(r)$ can be written in the form

$$v(r) = \frac{\Gamma}{2\pi} f(r) \quad (1)$$

where Γ is known as the circulation, r is the radial distance from the vortex center and f takes different forms depending on the vortex model one chooses. Due to viscous effects, f normally varies as r near the center and falls off like $1/r$ away from the center, i.e., it behaves like a rotating solid body near the center and like a potential vortex far away. The change over from solid body rotation to potential flow happens over some length. One can typically define a “core” radius which reflects this change over. In literature, many forms for f are found. In the case of a Rankine vortex, f varies as r over a distance a and falls off like $1/r$ beyond it. For a Gaussian vortex we have ($f = f_{gv}$)

$$f_{gv}(r) = \frac{1 - e^{-r^2/a^2}}{r} \quad (2)$$

In Lamb-Oseen model, the “core” radius a is allowed to decay with time due to viscous effects. In the present study, we employ Burnham-Hallock model for which $f=f_{bh}$ is given by

$$f_{bh}(r) = \frac{r}{r_c^2 + r^2} \quad (3)$$

where r_c denotes the “core” radius. Incidentally, when we consider the limit of $r \rightarrow 0$, the “core” size of Gaussian vortex and that of Burnham-Hallock vortex become identical. The trailing vortex pair(s) of any aircraft move under their own influence and are known to be unstable. The vortices eventually die out owing to turbulent decay as well as a number of physical processes such as vortex breakdown, linking and so on. Estimate of vortex wake life time is an important issue for transport aircraft. But for the present, since one is interested in close combat scenario, it is generally safe to model wake as consisting of a pair of “stationary” vortices that may possibly undergo decay. Then, we have on hand essentially the vortex strength Γ , the core size and the inter-vortex distance as primary defining parameters for the wake. In principle, any admissible form for the function $f(r)$ should suffice. For our purpose, we choose the Burnham-Hallock model. Straightforward application of the Joukowski theorem gives

$$\Gamma = \frac{W}{\rho V_\infty b_v} = \frac{n_z m g}{\rho V_\infty b_v} \quad (4)$$

where we assume that the separation between the two vortices is given by

$$b_v = \pi \frac{b}{4} \quad (5)$$

Here, n_z is the g-loading, m is the aircraft mass, g is the acceleration due to gravity, ρ is the ambient air density, V_∞ is the flight speed and b is the span. The vortical distance given above is strictly true for elliptical load distribution though it is a reasonable assumption for the present case.

3.1. Wake structure, vortex decay and modes of encounter

The wake structure assumed for the present case is shown in Figure 2. Since we assume infinitely straight wake vortex filaments, the induced flow is pure two-dimensional as shown. Any encounter can be thought of as combination of three fundamental modes, numbered 1, 2 and 3 in Figure 2. In mode 1, the penetrator (or follower) enters a core resulting in induced roll while in mode 2 it enters between the two aircraft resulting in loss of height due to the downwash. Mode 3 is crosswise entry which is

normally hazardous to the structure. For the present simulation, arbitrary encounters are considered. Vortices normally decay due to viscous effects. In the near wake, normally the decay is due to molecular viscosity while far wake can rapidly decay due to turbulence. To estimate absolute safe distance, suitable decay models, such as P2P [6], will be considered later. It is also possible to use a suitable RANS solver to estimate the wake vortex decay. Molecular viscosity normally results in expansion of the core size without much effect on the total circulation while turbulent decay results in loss of circulation. Next we consider the effect of this wake on the following aircraft and its resultant motion.

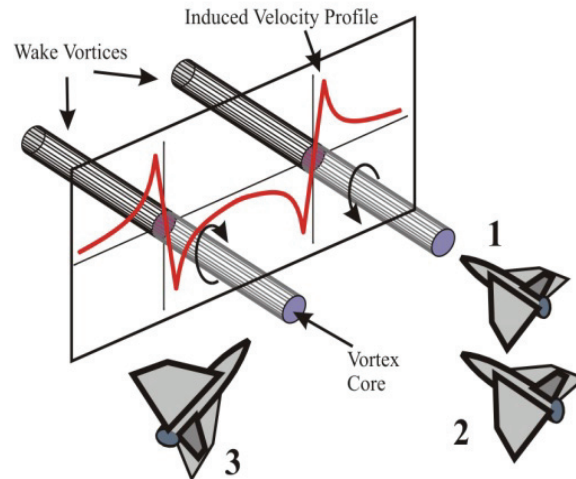


Figure 2. Schematic showing wake structure consisting of two counter-rotating straight vortices and the resultant induced velocity in a typical cross-sectional plane. Three fundamental encounter modes are depicted (numbered 1, 2 and 3).

4. INCREMENTAL AERODYNAMIC EFFECTS DUE TO WAKE

The interaction of the wake with the follower aircraft is typically modeled using either strip theory methods [8] or vortex lattice approach [4, 9]. Here we follow the strip theory approach. For this purpose, we divide the aircraft into different parts on which a local effect of the wake are determined. The local effect for each part is accounted for by adding the wake velocity to the undisturbed free stream resulting in change of flow vector. Since we choose just one representative point per part for wake velocity, one chooses the part so that the wake velocity variation over this part is small. The induced wake vector can be resolved along the body axes. One component alters the local angle of attack (local α) while another changes the local sideslip (local β). These are dominant effects. The third component changes local airspeed (V). This effect is usually small. However, the induced components are a strong function of entry geometry. The manner in which the aircraft is divided into different pieces which we call boxes should be based on the assumption that the induced wake velocity variations over those boxes is small. In the present case we choose the following (See Fig. 3):

- Box 1: Forebody – from nose tip to wing attachment point.
- Box 2: Aft fuselage – entire aft fuselage to the nozzle.
- Box 3: Left wing – outward from the fuselage attachment to inboard elevon end.
- Box 4: Left wing – outward from the inboard elevon end till wing tip.
- Box 5: Right wing – outward from the fuselage attachment to inboard elevon end.
- Box 6: Right wing – outward from the inboard elevon end till wing tip.
- Box 7: Fin.

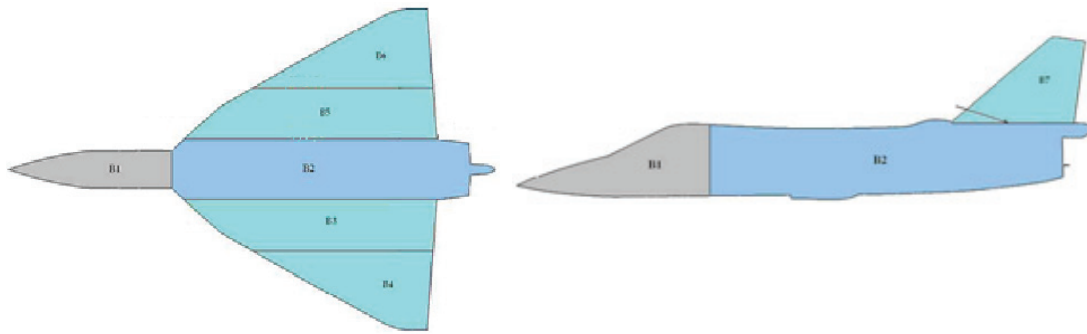


Figure 3(a). Box Definition (Plan View). Figure 3(b). Box Definition (Side View).

4.1. CFD based component level aerodynamic data generation

A well validated CFD solver is used to compute the complete surface pressure distribution on the vehicle as a function of α , β , Mach number (Mach) and slat deflection. By integrating over each of the above boxes, aerodynamic data for each of the six aerodynamic coefficients is generated in the following functional form:

$$\begin{aligned} C_{X_i}(\alpha, \beta, Mach, Slat), \quad C_{Y_i}(\alpha, \beta, Mach, Slat) \\ C_{Z_i}(\alpha, \beta, Mach, Slat), \quad i = 1, \dots, N \end{aligned} \quad (6)$$

$$\begin{aligned} C_{\ell_i}(\alpha, \beta, Mach, Slat), \quad C_{m_i}(\alpha, \beta, Mach, Slat) \\ C_{n_i}(\alpha, \beta, Mach, Slat), \quad i = 1, \dots, N \end{aligned} \quad (7)$$

where N is the number of boxes which is 7 in the present case. The first three coefficients are the forces along the body axes and the next three are the respective moments. In this manner it is possible to consider the effect of the local α , local β and local Mach number on each of the seven boxes arising out of the induced wake vortex field of the leader aircraft. It should be noted that the wake effect is computed on just one control point per box. For this, we choose the center of pressure for each box. Next section describes in detail the method of estimating aerodynamic interaction. The present method differs from the approach used in [4] and [9]. Since the wake encounter happens rather fast, it is not considered necessary to use detailed analysis as in [7].

4.2. Incremental aerodynamic interaction model implementation

The aerodynamic interaction model based on the CFD data for the wake encounter studies is implemented in the six degrees of freedom simulation model. The block diagram in fig 4 shows its interaction with the basic aerodynamic model.

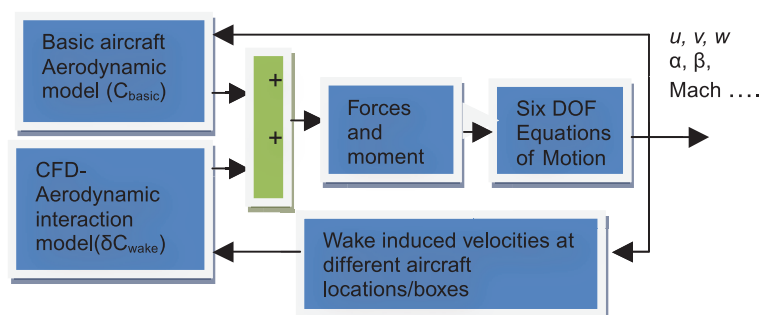


Figure 4. Wake effects on aerodynamics.

In figure 4, C_{basic} denotes all the six aerodynamic force and moment coefficients for the basic aircraft as developed from the wind tunnel data and validated by flight tests, whereas δC_{wake} denotes incremental component of all the six aerodynamic force and moment coefficients due to the incremental induced velocities of the wake as each control point summed over the seven boxes.

4.3. Computation of incremental force and moment coefficients due to wake from CFD data

The steps involved in computing the incremental force and moment coefficients due to wake based on the CFD data are enumerated below:

1. From the 6 DOF simulation model, obtain α , β , Mach, u , v , and w of the aircraft entering the wake.
2. For the above α , β , Mach, interpolate and obtain component level force and moment coefficients from the integrated CFD data. This represents the base CFD data over which the increment has to be calculated.
3. $C_{ref} = C_{b1ref}(\alpha, \beta, \text{Mach, slat}) + C_{b2ref}(\alpha, \beta, \text{Mach, slat}) + C_{b3ref}(a, b, \text{Mach, slat}) + C_{b4ref}(\alpha, \beta, \text{Mach, slat}) + C_{b5ref}(\alpha, \beta, \text{Mach, slat}) + C_{b6ref}(a, b, \text{Mach, slat}) + C_{b7ref}(\alpha, \beta, \text{Mach, slat})$
4. The control point for aircraft components (boxes) is interpolated as a function of Mach number.
5. Convert the control points (for all the boxes, arranged in an array) from body to inertial frame and add it with CG to obtain the position vector.
6. $\vec{r} = \vec{r}_{CG} + [\text{Inertial to body DCM}] \vec{r}_{Control\ point}$
7. Determine the local velocity at the location using Burnham-Hallock model.
8. The Burnham-Hallock model returns induced velocity in the inertial frame for all the seven aircraft components.
9. Convert the induced velocity for all the seven components from inertial frame to body frame using DCM.

$$10. \begin{bmatrix} u_i \\ v_i \\ w_i \end{bmatrix} = [\text{Inertial to body DCM}] \begin{bmatrix} V_{ni} \\ V_{ei} \\ V_{di} \end{bmatrix}$$

where $i = 1$ to number of aircraft components/boxes.

11. Add induced velocities to aircraft body velocities and obtain the resultant velocities at each control point.
12. $\begin{bmatrix} u_r \\ v_r \\ w_r \end{bmatrix} = \begin{bmatrix} u \\ v \\ w \end{bmatrix} + \begin{bmatrix} u_i \\ v_i \\ w_i \end{bmatrix}$
13. From the resultant velocities, compute α , β , Mach at each control point.
14. Compute, the component level force and moment coefficients for the above α , β , Mach for each of the seven boxes.
15. $C_{new} = C_{b1new}(\alpha, \beta, \text{Mach, slat}) + C_{b2new}(\alpha, \beta, \text{Mach, slat}) + C_{b3new}(a, b, \text{Mach, slat}) + C_{b4new}(\alpha, \beta, \text{Mach, slat}) + C_{b5new}(\alpha, \beta, \text{Mach, slat}) + C_{b6new}(a, b, \text{Mach, slat}) + C_{b7new}(\alpha, \beta, \text{Mach, slat})$
16. Compute delta force and moment coefficients due to wake induced velocity profile alone.
17. $\delta C_{wake} = C_{new} - C_{ref}$
18. Subsequently, proceed as per block diagram in figure 2.

The basic CFD data was also compared with flight test validated wind tunnel database and the match was found to be good.

5. WAKE EFFECTS ON AIR DATA SENSORS

The wake induces local flow that affects each air data sensor differently owing to non-uniformities over the aircraft scale. Local effects and global effects are connected through two algorithms described below.

5.1. Inverse model

The inverse model simulates the local values of Angle-of-Attack (AoA), Sideslip Angle (SSA) and pressure sensor seen locally as a function of the free stream parameters. It takes into account the position error correction for different sensors due to the presence of aircraft body in the flow field as

well as the kinematic effects.

5.2. Forward model

This algorithm includes the calculation of free stream values from different sensor values measured locally and the failure logic for different sensors, in the event of a mistrack between two sensor readings based on threshold values. The forward ADS model is identical to the algorithm implemented in the Air Data Computers (ADCs) on the aircraft.

6. COMBINED WAKE EFFECTS ON AERODYNAMICS AND AIR DATA SENSORS WAKE EFFECTS ON AIR DATA SENSORS

In Figure 5, the schematic of the complete model assembled to study the wake vortex encounter consisting of the aircraft six degree of freedom model, air data system and the flight control laws is illustrated. A typical simulation result is shown in Figure 6a-6c. In this simulation, the leading aircraft is assumed to be flying at about 0.65 Mach, 4.5 Km altitude with a normal load of 6 g. The following aircraft encounters the right wake of this aircraft from behind in a 5 degree climb at 1 g at a distance of 300 m behind. The initial location of this aircraft is chosen such that the vortex core is encountered at about 2 seconds into the simulation.

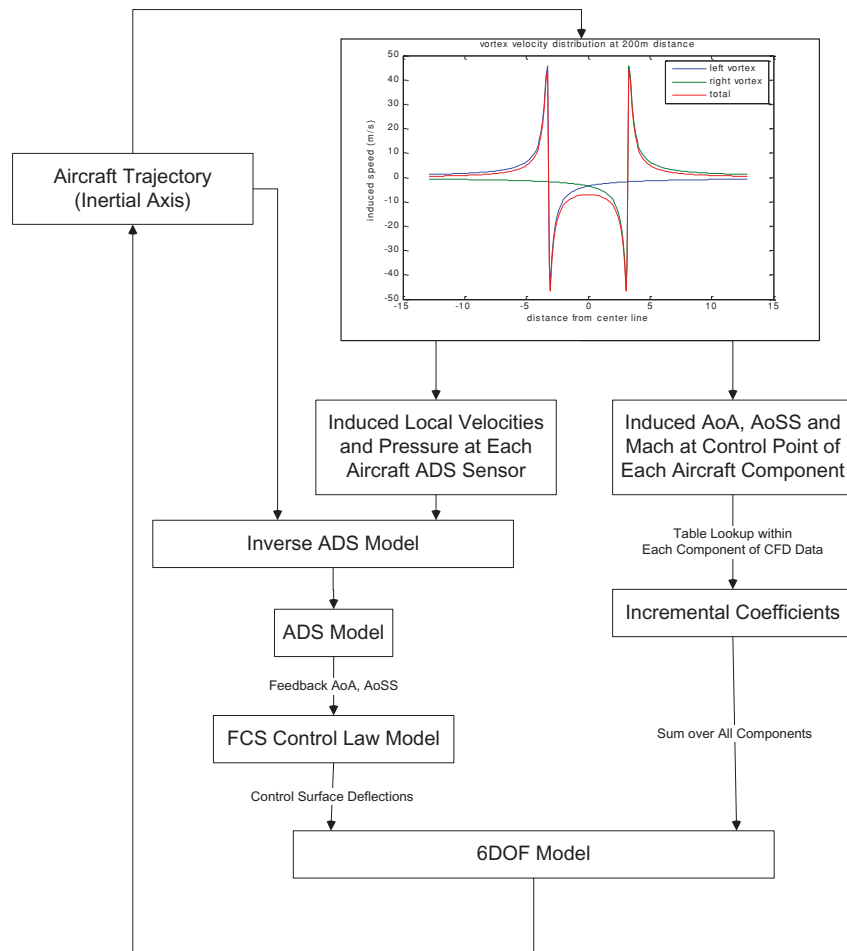


Figure 5. Total wake effects on ADS and aerodynamics.

In Figure 6a we see that as the follower aircraft passes through the wake vortex of the leader, it experiences an imposed upward velocity which sharply increases the angle of attack for a short duration which in turn increases the normal acceleration. There is also a sharp change in the associated pitch rate.

In Figure 6b we notice that the follower aircraft sees a rapid buildup of roll in excess of 200 deg/sec and yaw rate in excess of 15 deg/sec as it passes through the wake vortex. The angle of sideslip is also seen to undergo a variation between -5 deg to about 2.5 deg. The lateral acceleration also exceeds +/- 1g.

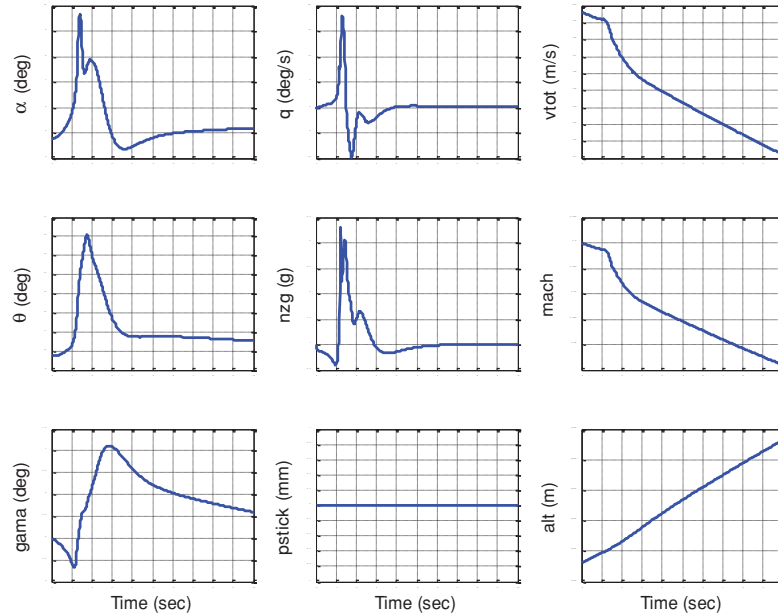


Figure 6(a). Longitudinal Response of the Fighter Aircraft to right vortex encounter at 300m.

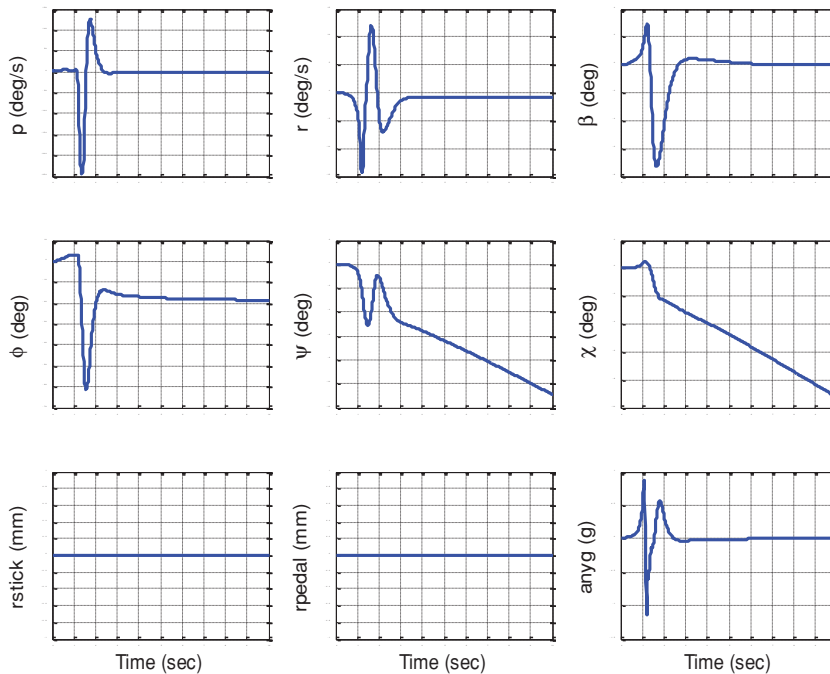


Figure 6(b). Lateral-Directional Response of the Fighter Aircraft to right vortex encounter at 300m.

Figure 6c shows the response of the Air Data computed angles of attack, sideslip, static and dynamic pressures. Clearly, the Air Data System filters out a significant part of the local velocity perturbations in the measurements due to wake.

In Figure 6d we see the control surface deflections due to the reaction of the control laws to the transient deviations in the angle of attack feedback and the aircraft inertial accelerations and rates due to the wake-encounter.

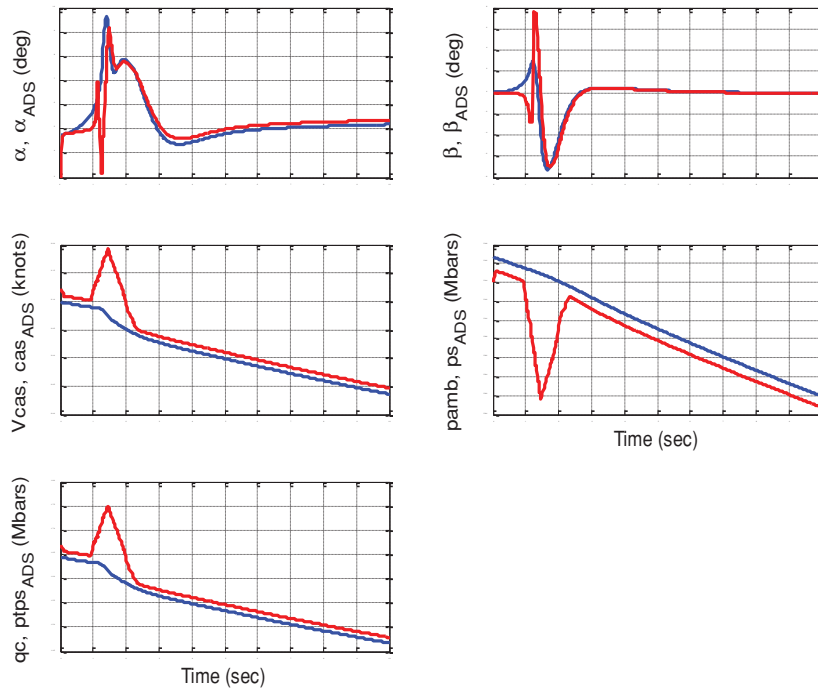


Figure 6(c). Response of the air data system of the fighter aircraft to right vortex encounter at 300 m (Red: 6DOF value, Blue: ADS computed value).

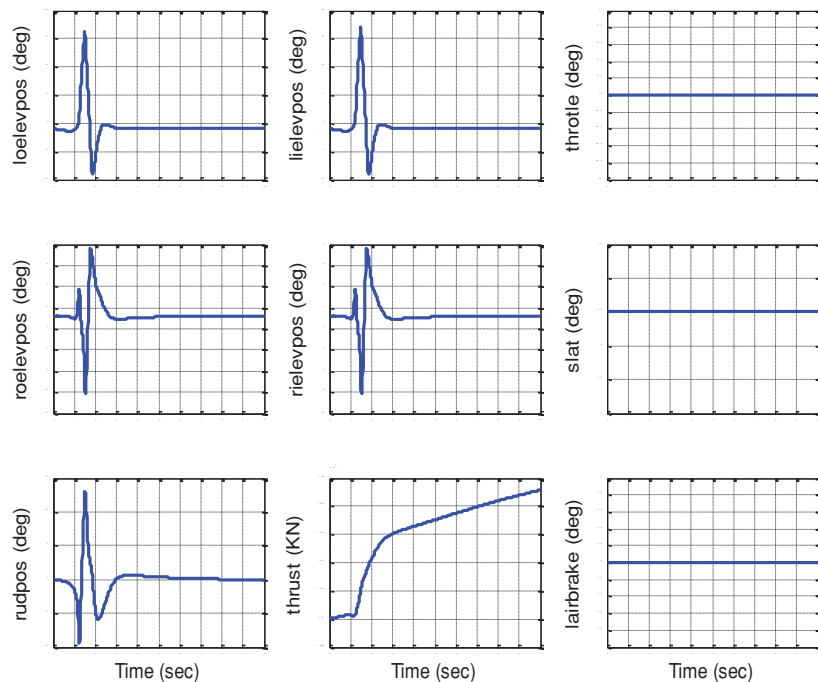


Figure 6(d). Response of the control surfaces of fighter aircraft to right vortex encounter at 300 m.

CONCLUSIONS

A rigid body simulation is set up for predicting the effects of a wake encounter of one high performance fighter aircraft with another. The approach similar to strip theory is used. Results of simulations are presented. The results show that the excursions in angle of attack, side slip angle and other aerodynamic quantities can be significant due to wake. This model will be further validated against flight test results in the near future. The methodology developed provides a sound framework to obtain wake encounter clearance for a fighter aircraft.

REFERENCES

- [1] Mudkavi, Vidyadhar Y. and Dutta, P. K., Aircraft Wake Vortex Modelling, Special Publication, SP 9224, National Aerospace Laboratories, Bangalore. December 1992.
- [2] Rossow, Vernon J., Lift-generated vortex wakes of subsonic transport aircraft, *Progress in Aerospace Sciences*, Vol. 35, Issue 6, August 1999, Pages 507-660.
- [3] Gerz, Thomas, Holzäpfel, Frank, Darracq, Denis, Commercial aircraft wake vortices, *Progress in Aerospace Sciences*, Volume 38, Issue 3, April 2002, Pages 181-208.
- [4] Yngve C-J. Sedin, Ingemar Gråsjö, Erik Kullberg, Roger Larsson, A model for simulation of flight passages through trailing tip vortices, Paper ICAS 2002-7.9.3.
- [5] Hans-Erik Hanson, JAS 39 Gripen Wake vortex penetration flight testing, 17th SFTE(EC) Symposium, 12-14 June 2006.
- [6] Holzäpfel, Frank, "Probabilistic Two-Phase Wake Vortex Decay and Transport Model," *J. Aircraft*, Vol. 42, No. 2, 2003.
- [7] Deborah Saban, Wake vortex modeling and simulation for air vehicles in close formation Flight. Ph.D thesis, School of Engineering, Cranfield University, 2010.
- [8] Pete, K. R., Smith, S. T., and Vicroy, D., *Model Validation of Wake-Vortex/Aircraft Encounters*. AIAA Paper 2000-3979, August 2000.
- [9] Lampe, T.; Sedin, Y.; Weinerfelt, P. (2005) Flight Test Verification of a Wake Vortices Model. In Flight Test – Sharing Knowledge and Experience (pp. 4-1 – 4-16). Meeting Proceedings RTO-MP-SCI-162, Paper 4. Neuilly-sur-Seine, France: RTO. Available from <http://www.rto.nato.int/abstracts.asp>.
- [10] Atilla Dogan and Timothy A Lewis, Flight data analysis and simulation of wind effects during aerial refueling, *Journal of Aircraft*, Vol. 45, No 6, November-December 2008.
- [11] Muller, B. and Hinterwaldner, M., Wake penetration-A tumultuous farewell of 1st Typhoon prototype aircraft, 17th SFTE (EC) Symposium, 12-14 June 2006.